LAWRENCE
LIVERMORE
NATIONAL
LABORATORY

LLNL-JRNL-404698

Optimization of Optical and Electronic properties of Carbon Fullerenes: Symmetry-Reduced C60 and Dumbbell-Like Novel Structures

M. R. Manaa

June 16, 2008

Journal of Computational and Theoretical Nanoscience

Disclaimer

Optimization of Optical and Electronic properties of Carbon Fullerenes: Symmetry-Reduced C_{60} and Dumbbell-Like Novel Structures

M. Riad Manaa

Lawrence Livermore National Laboratory
Energetic Materials Center
P.O. Box 808, L-282
Livermore, California, 94551

Invited contribution to be submitted to Journal of Computational and Theoretical Nanoscience

Abstract:

Using quantum chemical density functional calculations, we study two possible pathways for manipulating the optical and electronic properties of all-carbon fullerenes structures. In the first, the optical properties of C_{60} are shown to be enhanced via reduction of the perfectly spherical I_h symmetry structure to energetically feasible lower symmetries. A D_{3d} symmetry structure of C_{60} proved to be 39 meV lower in energy than the I_h conformation. This reduction in symmetry activates otherwise silent modes in the IR and Raman spectra, possibly achievable via solvation effects. In the second pathway, fusing a building block of an-all carbon hexagonal unit as a connector between two C_{60} cages is considered. Optimizations on a resulting series of dumbbell-like structures, molecular C_{126}, C_{132}, C_{138}, C_{144}, and C_{180}, impart distinct variation in the electronic properties of these novel structures with size. These structures are further shown to support stable anionic radical forms.

I. Introduction.

Optimization of the electronic, optical, and magnetic properties of nanomaterials to a desired outcome is recognized as a prime objective for major advancements in nanotechnoloy. [1] For example, new developments in carbon fullerene doping have attracted much interest due to expectation of novel chemical and physical properties when varying the amount of dopant in fullerene cages. [2] Several doping methods currently exist for altering the electronic structure of the parent fullerenes. [3] These methods of synthesis are accomplished either by introducing dopant species to surround the fullerene cage, or by the inclusion of ions inside it. Another approach is the substitution of one or more of the carbon atoms with dopants. $C_{48}N_{12}$ is an example of several recently synthesized molecular systems in which the carbon atoms in the C_{60} cage are replaced either by nitrogen or boron counterparts. [3-7] Compared to C_{60}, $C_{48}N_{12}$ showed an enhancement of its second hyperpolarizibility by about 55%, making it a good candidate for optical limiting applications. [8] It was also shown that $C_{48}N_{12}$ could be used to build diamagnetic materials due to its enhanced diamagnetic shielding factor in the carbon atom. [9] Moreover, computation of electron acceptor $C_{48}B_{12}$ and donor $C_{48}N_{12}$ demonstrated these materials to be promising components for molecular rectifiers, carbon nanotube-based *n-p-n* (*p-n-p*) transistors and *p-n* junctions. [10-11]

Aside from introducing heterogeneity into the system, it is possible to fine-tune the electronic properties by manipulating the structural attributes in a homogeneous nanomaterials. Such is the case in carbon nanotubes, which could be made as metals

or semiconductors, depending on the diameter and the chirality of the nanotube. [12] In this work, our aim is to explore altering the optical and electronic properties of carbon fullerenes *without* the introduction of a foreign agent or dopant. Using quantum chemical calculations, we establish two possible pathways to manipulate and optimize the optical and electronic properties of all-carbon fullerenes structures. In the first, the optical properties of C_{60} are shown to be enhanced via reduction of the perfectly spherical I_h symmetry structure to energetically feasible lower symmetries. [13] Experimentally, this symmetry reduction is thought to be demonstrated for C_{60} in benzene, toluene, and CS_2 solutions. [14, 15] In the second, we consider adding a building block, an-all carbon hexagonal unit, as a connector between two C_{60} molecules. Optimizations on such a series of dumbbell-like structures of increasing size, with molecular formulas C_{126}, C_{132}, C_{138}, C_{144}, and C_{180} (figure3), show distinct variation in the electronic properties of these novel structures that they might serve as new optoelectronic materials.

II. Enhanced Optical Activity of Symmetry-Reduced C_{60}.

Ever since its discovery in 1985, the celebrated geodesic cage structure of the C_{60} molecule has become one of the rare examples of prefect symmetry structures in nature. [16] A truncated icosahedron, in which all sixty vertices are equivalent, C_{60} possesses the full I_h symmetry, thus making it the most spherical of all known molecules. [17] Inherent in this high symmetry is an intricate network of electron-phonon coupling, evident in phonon progressions and vibronic peak broadening, [18] and resulting in structural distortions of neutral C_{60} in the presence of solvent. [14,15,19] Within the I_h symmetry group, there are forty-six distinct vibrational

frequencies, with the following symmetries: $\Gamma = 2A_g + 3T_{1g} + 4T_{2g} + 6G_g + 8H_g + A_u + 4T_{1u} + 5T_{2u} + 6G_u + 7H_u$. Ten modes are Raman-active and four are IR-active (in the first order), while the remaining 32 modes are optically silent. [12] As the symmetry of C_{60} is reduced from I_h to, say, D_{3d}, the number of distinct vibrational modes increase to 116, having the following symmetries: $\Gamma = 16A_{1g} + 13A_{2g} + 29E_g + 14A_{1u} + 15A_{2u} + 29E_u$. Symmetry-reduced structures of C_{60} would activate some of the otherwise silent I_h modes, which could then be amenable to experimental verification as in resonance Raman scattering. [20-21]

We performed quantum chemical calculations, at the density functional B3LYP and BPW91 levels, [22-26], and with two different basis sets, on symmetry constrained structures of C_{60}: I_h, T_h, D_{5d}, D_{3d}, and S_6. Results of optimization within these symmetry constraints proved, consistently, that the D_{3d} structure is the lowest in energy at all levels of theory, being about 35-39 meV even lower than the I_h symmetry constrained molecule, as listed in Table I. Although for practical purposes these structures could be considered as energetically degenerate, a new assignment of the ground electronic state of C_{60} should now be as the $^1A_{1g}$ state of D_{3d} symmetry.

Figure 1 shows the optimized structure of the lowest energy D_{3d} symmetric C_{60} at the B3LYP/6-31G* level of computation. Within this symmetry, there are 10 unique carbon-carbon bonds. Optimization of the I_h structure at the same level yields 1.454 and 1.396 Å for the two unique C-C bonds, to be compared with neutron scattering average values of 1.455 and 1.391 Å. [27] Note that the diffraction results are averages for three sets of values comprising of fifteen measured bonds. The D_{3d} optimized structure has four short bonds in the range 1.396-1.410 Å, and six long

bonds within the range 1.447-1.459 Å. These values illustrate only small distortions from the I_h structure, consistent with the slight energy change reported in Table I. The C_{60} molecule transitions from a spherical top form in the I_h symmetry to a prolate symmetric top form in the D_{3d} symmetry structure. This symmetry lowering thus produces a slight, anisotropic change in the quadrupole moment from σ= -324.09 (Debye-Å) in I_h symmetry, to $\sigma_{XX} = \sigma_{YY}$ = -324.09, σ_{ZZ} = -324.15 in the D_{3d} structure, as calculated at this level of theory. It should be noted that a change in the quadrupole moment has been predicted in order to account for an observed solvatochromism shifts of C_{60}. [28]

Re-organization among these various symmetry structures can thus occur easily through tunneling, when exposed to external perturbations such as solvent environment. It is interesting to note that similar D_{3d} and D_{5d} lower energy structures; Jahn-Teller distortions in the C_{60} anion radical have been predicted. [29] Transitions between neutral and anionic C_{60}, both of which are now geometrically of D_{3d} symmetry, is very favorable according to the Franck-Condon principle. Further, with the full vibrational structure of I_h, D_{3d}, and D_{5d} symmetry calculated, the D_{3d} structure has the largest zero-point energy of 10.20 eV, compared with 10.18 eV for the I_h structure at the B3LYP/6-31G* level.

A consequence of symmetry lowering is the splitting of electronic molecular energy levels. The highest occupied state of C_{60} in I_h symmetry is the completely occupied, five-fold degenerate h_u state, while the lowest unoccupied state is the three-fold degenerate t_{1u} state. The energy band gap between the HOMO and LUMO states is calculated to be 2.76 eV at the B3LYP/6-31G* level. In D_{3d} symmetry, the h_u state

splits into one A_{2u} and two doubly degenerate E_u states, separated by 24 cm^{-1}. The t_{1u} LUMO state splits into A_{2u} and E_u, with the A_{2u} mode being 18 cm^{-1} lower in energy at this level of calculation. The HOMO-LUMO separation is then an E_u-E_u gap in D_{3d} symmetry, equal to that of the I_h symmetry. The level splitting in this symmetry causes both the HOMO and LUMO to be shifted higher in energy by an almost similar magnitude.

The calculated Raman scattering activities for the I_h and D_{3d} symmetry structures at the B3LYP/6-31G* level is shown in Figure 2. In I_h symmetry, two A_g and eight H_g fundamental vibrational modes are Raman active, altogether with combination and overtone modes, have been experimentally assigned for the solid phase. [30] The calculated and measured frequencies are shown to be in good agreement. In D_{3d} symmetry, the H_g mode correlates with one A_{1g} and two E_g modes. The calculated Raman activities show very small splitting of the active modes: the lowest frequency H_g mode at 265 cm^{-1} splits into two modes at 266 and 267 cm^{-1}. Similar splitting for all other active modes at 434, 715, 786, 1125, 1275, 1453, and 1616 cm^{-1}, with a frequency shift of at most 3 cm^{-1} is calculated for the D_{3d} symmetry structure. Similar results have been obtained for the calculated Raman activities of the D_{5d} structure, for which the H_g mode splits into the A_{1g}, E_{1g} and E_{2g} modes. For this structure, the only active modes in the region of up to 500 cm^{-1} are determined for the bands at 266, 436, and 497 cm^{-1}.

The Raman spectrum of D_{3d} C_{60} in Figure 2 shows a weak band at 1539 cm^{-1}. This is due to the activation of otherwise silent mode, and of A_{1g} character. Two much weaker E_g modes also appear at 1538 cm^{-1}. Experimentally, a silent G_g band at

1525 cm^{-1} has been assigned in I_h symmetry. In D_{3d} symmetry, this mode should correlate with the A_{1g}, A_{2g}, and E_g modes, of which only the A_{1g} and E_g are Raman active. The appearance of this band in a region significantly removed from other fundamentals should, therefore, be a Raman signature for the existence of this structure and could be discerned in high-resolution Raman spectroscopy of C_{60} in the gas-phase. The existence of two H_g overtones in the same region, however, could prove its identification a challenging case indeed. [30]

The four IR-active T_{1u} modes in the I_h symmetry are calculated at the B3LYP/6-31G* level to have frequencies of 532, 587, 1212, and 1459 cm^{-1}. These also compare well with the experimental measurements of 527, 576, 1183, and 1430 cm^{-1}. [31] The small distortions into D_{3d} symmetry shift these frequencies to higher values of an utmost 5 cm^{-1}. Two weak bands are activated: one with frequencies of 541, 543 cm^{-1}, and a weaker still band at 1465 cm^{-1}. The first could be attributed to the I_h H_u silent mode at the experimentally assigned 563 band, while the second emanates from the silent G_u band, appearing with frequency of 1446 cm^{-1}. [31] Previous assignments of weak IR modes, specifically in the high frequency region, as due to combination modes caused by anharmonicity may well in fact be originated from a geometrical change of C_{60} to the lower D_{3d} symmetry. [32]

III. Dumbbell-Like Novel Structures.

The discovery of polymerized C_{60} has ignited an interest in the subject of electronic interactions between adjacent C_{60} cages. [33,34] Dimeric form of C_{60} has received a particular attention as a model of fullerene polymers, with interest in

understanding how the close contact of curved π–conjugated structures might influence the electronic properties of the overall cluster. One early example was the synthesis of an odd-numbered fullerenes, C_{119} [35] and C_{121} [36,37]. In a related venue, ladder-shaped molecules featuring a series of fused cyclobutane rings (dubbed as ladderanes) have also been achieved [38], with expected unique electronic properties that they may serve as spacers to separate metals or functional groups for a possible new class of active optoelectronic materials.

Instead of a butane ring, consider a carbon hexagon, benzene-like unit (as in graphite, for example), to be a building block, when fused, for a series of connectors between two C_{60} cages. Since it is known that there is a bond between the bridgehead carbon atoms of a 6,6-junction, and not between a 6,5 junction, [39] the hexagon unit is fused to two six-membered rings of the C_{60} cages. We determine the variation in electronic properties, at the B3LYP/6-31G* level of computation. Mainly, we calculate the HOMO-LUMO gap, for a series of 1, 2, 3, 4, and 10 fused units, leading to structures shown in figure 3, of C_{126}, C_{132}, C_{138}, C_{144}, and C_{180}. Such structures might also be considered as closed-curved, fused ladderanes, creating a connector tube of various lengths between two buckyballs.

Optimization of these structures, all with D_{3h} symmetry, resulted in distinct carbon-carbon bonding characteristics. Within the C_{60} cages, C-C bond distances are similar to the ones reported for the I_h and D_{3d} structures discussed in the previous section and vary in length between the two values 1.40 and 1.45 Å, reflecting little or no perturbation. Within the hexagonal unit, however, the optimized C-C bonds are 1.52 and 1.54 Å, representing mainly single C-C bonds, very similar to what is found

in ethane (C_2H_6). The bridging bonds, either between the C_{60} and the hexagon unit, or between two adjacent hexagon units are further stretched to 1.60 to 1.62 Å. Such values represent a further weakening of inter-connector C-C bonds, the sort of highly compressed, inter-layer graphitic sheets. Finally, the length of the tube between two C_{60} in C_{180} is about 17.75 Å.

Table II lists the calculated HOMO-LUMO, gap and binding energies of the series C_{126}, C_{132}, C_{138}, C_{144}, and C_{180}, and compare them with that of C_{60}. The calculated binding energy decreases monotonically with the size of the carbon cluster, from 6.87 for C_{126} to 6.38 eV per atom for C_{180}. These values are 0.11 to 0.6 eV/atom less than that of C_{60}, suggesting that these structures are amenable to synthesis. While fusing the initial hexagon unit lowers the binding energy by 0.11 eV/atom, successive additions decreases this value further in comparison with C_{60}. As determined from the results in table II, the binding energy variation is 0.095 eV/atom per unit for C_{132}, 0.083 eV/atom per unit for C_{136}, and 0.06 per unit for C_{180}.

As for the electronic properties, the calculated energy gap between the HOMO and LUMO molecular orbitals for the series of structures are displayed in figure 4. We notice appreciable decrease, albeit non-monotonic, in the energy gap from that of C_{60}. The calculated gap for C_{60} is determined to be 2.76 eV, and is in agreement with the experimental value of 2.3±0.1 eV of the solid phase. [40] Thus, the level of computation with B3LYP/6-31G* gives a reasonable predictive capability, as noted previously on other spectroscopic properties such as Raman scattering. [41] The slight increase in the energy gap for C_{138} and C_{144} is due to a slight deviation of the C-C-C angle of two adjacent hexagon units from linearity (=176°). We note that all the

structures considered herein have a HOMO that is higher in energy than that of C_{60}, while the LUMOs are placed energetically lower. Thus, increasing the size of the fusing unit tends to lower the HOMO energy towards that of C_{60}, and pushing the LUMO away from that of C_{60} at the same time. This energetic ordering of the HOMO and LUMO levels accounts for a significant drop in the energy gap to 2.17 eV for C_{180}. Synthetic C_{180} is thus predicted to have a pronounced difference in electronic properties than C_{60}, and should at least be considered as semi-conductor. Whether further decrease in the band-gap due to increase in the size of the fused, connecting hexagon unit is possible, perhaps to eventual metallization, remains to be explored. Such a feat will undoubtedly demonstrates a clear pathway for a distinct manipulation of electronic properties as a function of size at the nano-scale level.

Finally, with both the HOMO and LUMO levels are negative for every member of the dumbbell-like structure in the series as shown in Table II, it is possible for each to support an anionic radical structure. Optimizations of such anionic structures were determined at the UB3LYP/6-31G* level of theory. Table III lists the relative energies of these anions with respect to their corresponding neutral counterpart. While little structural differences in bonding appeared to be the norm, we note the increase in the electronic separation of these anions from the neutral species as a function of size. Although this separation is on the order of the HOMO-LUMO gap separation in the neutral species, it is also indicative of stabilization effect for these anions as the size of fused unit is increased.

Acknowledgments:

This work was performed under the auspices of the U.S. Department of Energy by Lawrence Livermore National Laboratory under contract number DE-AC52-07NA27344.

Figures Caption:

Figure 1. (a) The optimized, symmetry – unique D_{3d} carbon-carbon bonds of C_{60} (in Å). X denotes the C_3 axis of symmetry. These unique centers are clearly indicated (shadows) in (b).

Figure 2. Calculated Raman scattering activities (in $Å^4$/a.m.u) of D_{3d} and I_h structures of C_{60}.

Figure 3. Optimized dumbbell-like structures of C_{126}, C_{132}, C_{138}, C_{144}, and C_{180}.

Figure 4. HOMO-LUMO separation (in eV) of C_{60}, C_{126}, C_{132}, C_{138}, C_{144}, and C_{180}.

Table I. Energetic of symmetry-constraints structures of C_{60}.

Method	**Total Energy**	**Relative Energy** [a]		
	I_h	D_{3d}	D_{5d}	S_6
B3LYP/6-31G*	-2286.173080	-34.7	-26.0	-30.4
B3LYP/cc-pVDZ	-2286.314164	-39.0	-30.4	-30.4
BPW91/6-31G*	-2286.069710	-39.0	-30.4	-30.4

[a] in meV relative to I_h structure.

Table II. DFT- B3LYP/6-31G* energetics and electronic properties of dumbbell structures (as in figure 3).

Structure	**HOMO (eV)**	**LUMO (eV)**	**Gap (eV)**	**Binding Energy** (eV/atom)
C_{126}	-5.775	-3.426	2.35	6.87
C_{132}	-5.815	-3.529	2.29	6.79
C_{138}	-5.834	-3.472	2.36	6.73
C_{144}	-5.850	-3.469	2.38	6.67
C_{180}	-5.896	-3.730	2.17	6.38
C_{60}	-5.986	-3.225	2.76	6.98

Table III. Calculated relative energies of radical anionic dumbbell structures.

Anion	Δ**E** (eV)
C_{126}^-	2.58
C_{132}^-	2.73
C_{138}^-	2.68
C_{144}^-	2.71
C_{180}^-	3.06

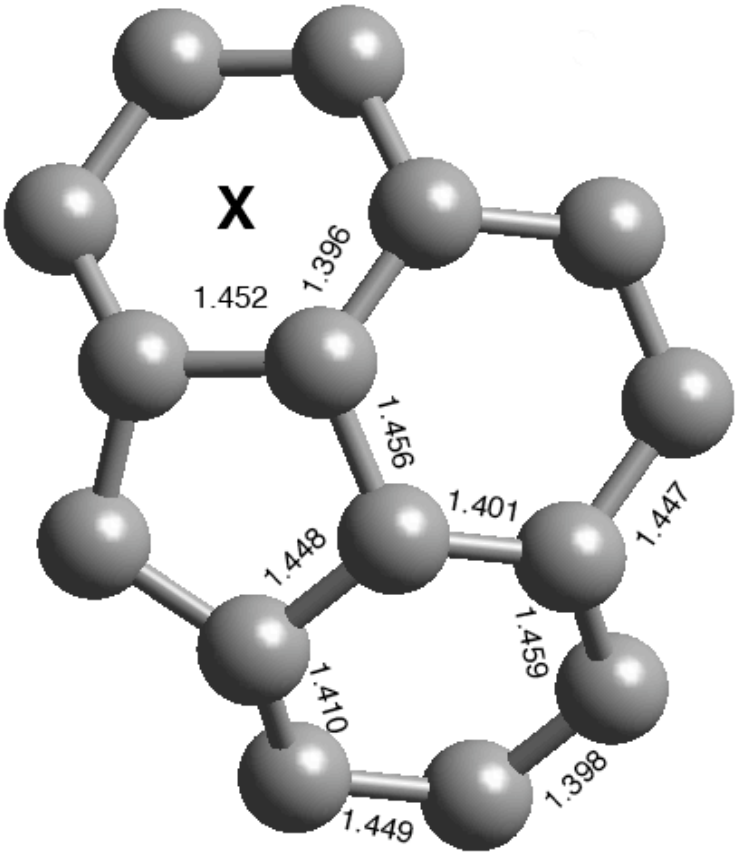

Manaa : Figure 1a.

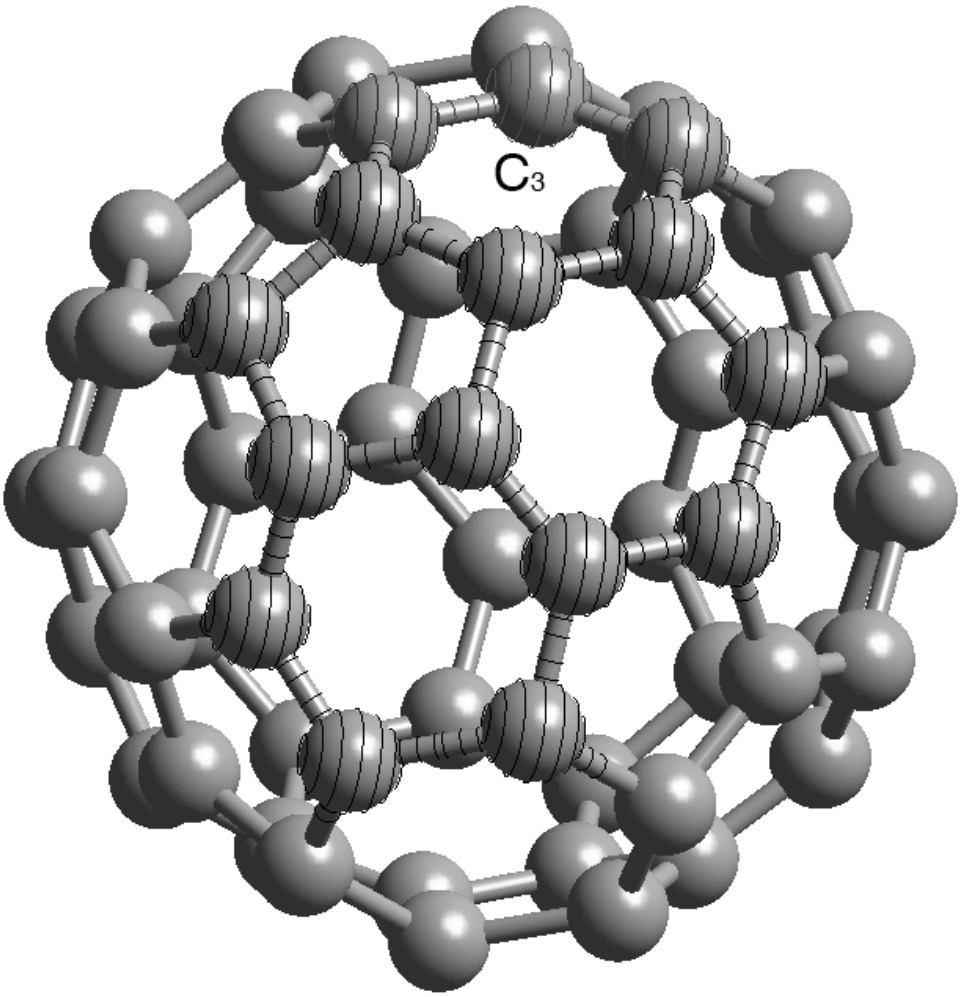

Manaa: Figure 1b.

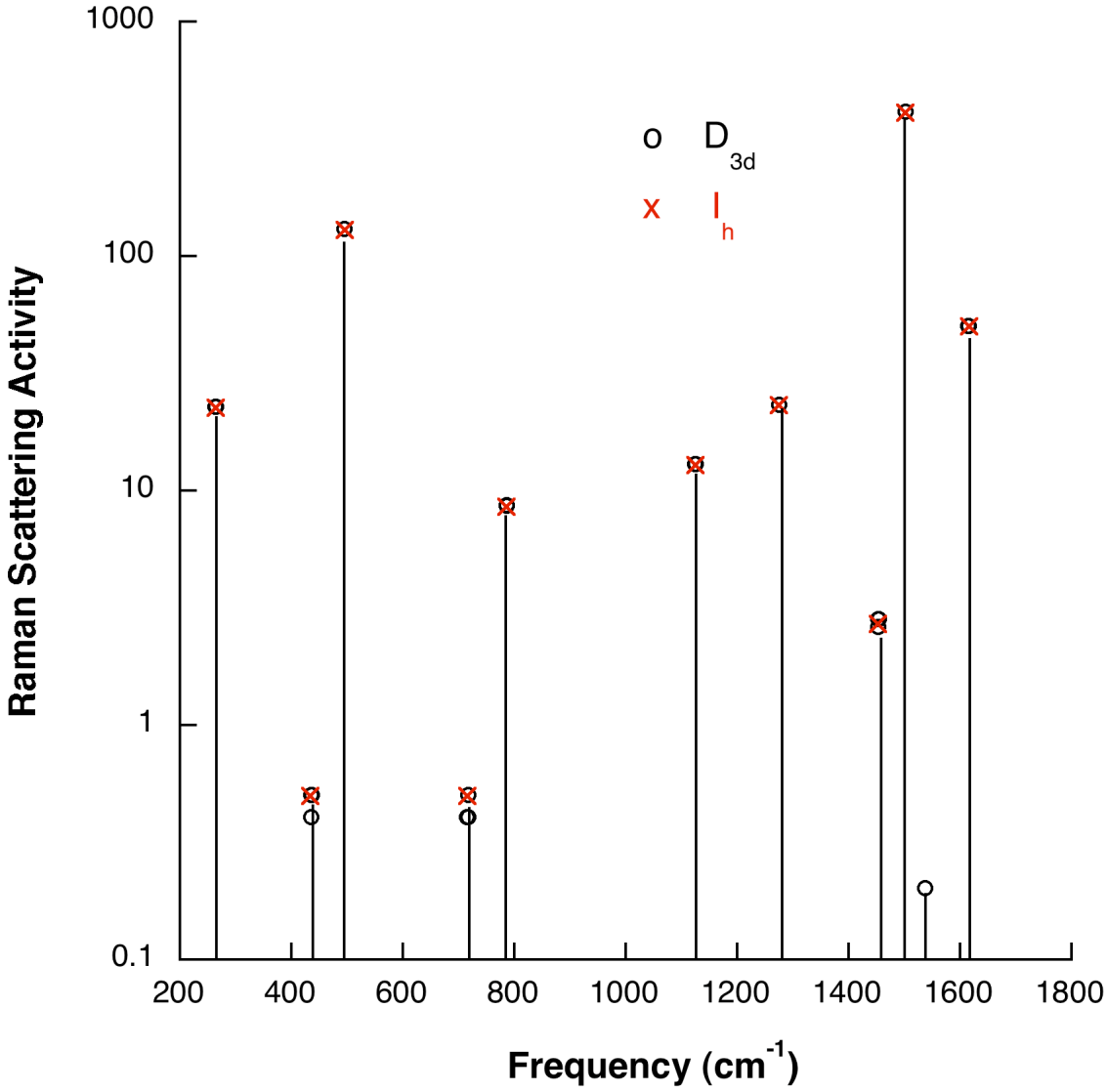

Manaa: Figure 2.

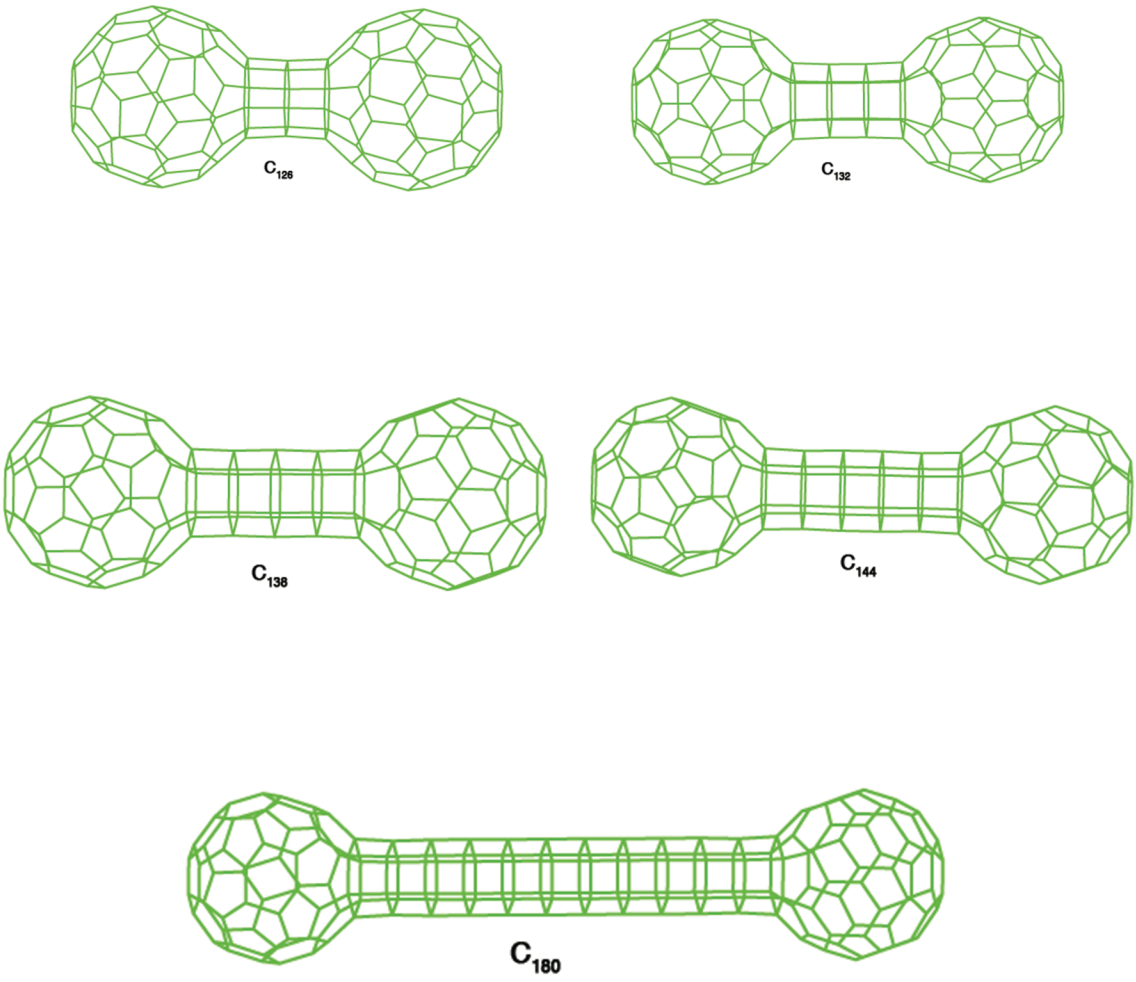

Manaa: Figure 3.

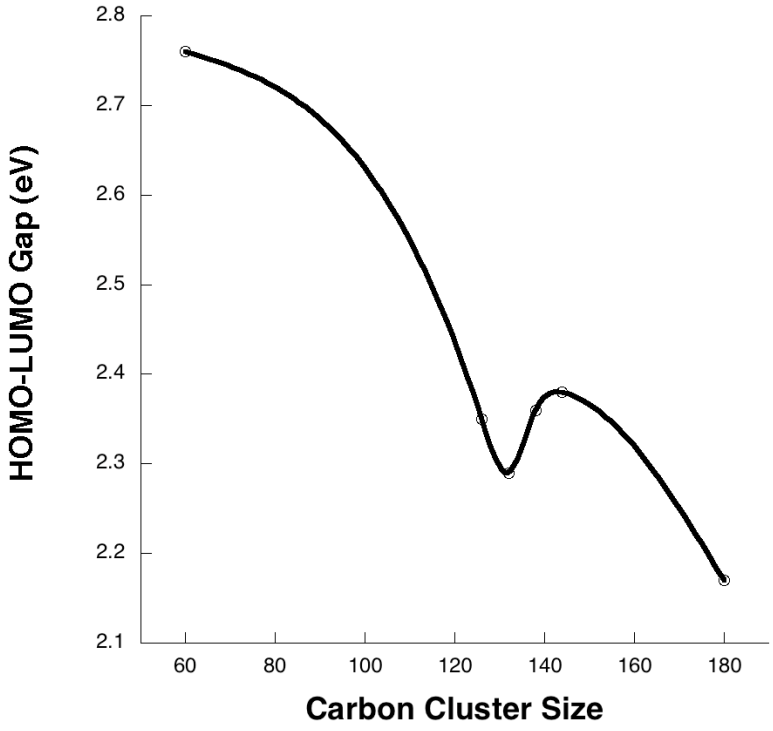

Manaa: Figure 4.

REFERENCES

[1] H.S. Nalwa (ed.), Handbook of Advanced Electronic and Photonic Materials and Devices, Nonlinear optical Materials, vol 9, Academic Press, New York, 2000.

[2] W. Andreoni (Ed.), The Physics of Fullerene-Based and Fullerene-Related Mateials, Kluwer, New York, 2000.

[3] R. H. Xie, G. W. Bryant, G. Sun, M. C. Nicklaus, D. Heringer, T. Frauenheim, M. R. Manaa, V. H. Smith Jr., Y. Araki, and O. Ito, J. Chem. Phys., 120 (2004) 5133.

[4] J. C. Hummelen, B. Knight, J. Pavlovich, R. Gonzalez, and F. Wudl, Science, 269 (1995) 1554.

[5] T. Guo, C. M. Jin, and R. E. Smalley, J. Phys. Chem., 95 (1991) 4948.

[6] L. Hultman, S. Stafström, Z. Czigany, J. Neidhardt, N. Hellgren, I. F. Brunell, K. Suenaga, and C. Colliex, Phys. Rev. Lett., 87 (2001) 225503.

[7] M. R. Manaa, D. W. Sprehn, and H. A. Ichord, J. Am. Chem. Soc., 124 (2002) 13990.

[8] R. H. Xie, G. W. Bryant, L. Jensen, J. Zhao, and V. H. Smith Jr., J. Chem. Phys., 118 (2003) 8621.

[9] R. H. Xie, G. W. Bryant, and V. H. Smith Jr., Chem. Phys. Lett., 368 (2003) 486.

[10] R. H. Xie, G. W. Bryant, J. Zhao, V. H. Smith Jr., A. Di. Carlo, and A. Pecchia, Phys. Rev. Lett,. 90 (2003) 206602.

[11] M. R. Manaa, Chem. Phys. Lett., 382 (2003) 194.

[12] M. S. Dresselhaus, G. Dresselhaus, and P. C. Eklund, Science of Fullerenes and Carbon Nanotubes, Academic Press Inc., San Diego, 1996.

[13] M. R. Manaa, Chem. Phys. Lett., 424 (2006) 139.

[14] S. H. Gallagher, R. S. Armstrong, P. A. Lay, and C. A. Reed, Chem. Phys. Lett., 248 (1996) 353.

[15] S. H. Gallagher, K. C. Thompson, R. S. Armstrong, and P. A. Lay, J. Phys. Chem. A,108 (2004) 5564.

[16] H. W. Kroto, J. R. Heath, S.C. O'Brien, R. F. Curl, and R. E. Smalley, Nature, 318 (1985) 162.

[17] H. W. Kroto, A. W. Allaf, and S. P. Balm, Chem. Rev., 91 (1991) 1213.

[18] C. Reber, L. Yee, J. McKiernan, J. I. Zink, R. S. Williams, W. M. Tong, D. A. Ohlberg, R. L. Whetten, and F. Diederich, J. Phys. Chem., 95 (1991) 2127.

[19] I. V. Rubstov, D. V. Khudiakov, V. A. Nadtochenko, A. S. Lobach, and A. P. Moravskii, Chem. Phys. Lett., 229 (1994) 517.

[20] S. H. Gallagher, R. S. Armstrong, P. A. Lay, and C. A. Reed, J. Am. Chem. Soc., 116 (1994) 12091.

[21] S. H. Gallagher, R. S. Armstrong, W. A. Clucas, P. A. Lay, and C. A. Reed, C. A. J. Phys. Chem. A, 101 (1997) 2960.

[22] A. D. Becke, J. Chem. Phys., 98 (1993) 5648.

[23] C. Lee, W. Yang, and R. G. Parr, Phys. Rev. B, 37 (1988) 785.

[24] A. D. Becke, Phys. Rev. A , 38 (1988) 3098.

[25] J. P. Perdew, and Y. Wang, Phys. Rev. B, 45 (1992) 13244.

[26] M. J. Frisch, et al., Gaussian 98, Rev. A.4, Gaussian, Inc., Pittsburgh PA, USA. 1998.

[27] W. I. F. David, R. M. Ibberson, J. C. Matthewman, K. Prassides, T. J. S. DennisJ. P. Hare, H. W. Kroto, R. Taylor, and D. R. M. Walton, Nature, 353 (1991) 147.

[28] S. H. Gallagher, W. A. Armstrong, P. A. Lay, and C. A. Reed, J. Phys. Chem., 99 (1995) 5817.

[29] N. Koga, and K. Morokuma, Chem. Phys. Lett., 196 (1992) 191.

[30] Z. H. Dong, P. Zhou, J. M. Holden, P. C. Eklund, M. S. Dresselhaus, and G. Dresselhaus, Phys. Rev. B, 48 (1993) 2862.

[31] K. A. Wang, A. M. Rao, P. C. Eklund, M. S. Dresselhaus, and G. Dresselhaus, Phys. Rev. B 48, (1993) 11375.

[32] J. Fabian, Phys. Rev. B, 53 (1996) 13864.

[33] A. M. Rao, P. Zhou, K. A. Wang, et al., Science, 259 (1993) 955.

[34] J. L. Segura, and N. Martin, Chem. Soc. Rev., 29 (2000) 13.

[35] R. S. W. McElvany, J. H. Callahan, L. D. Lamb, and D. R. Huffman, Science, 260 (1993) 1632.

[36] N. Dragoe, H. Shimotani, J. Wang et al., J. Am. Chem., 123 (2001) 1294.

[37] H. Shimotani, N. Dragoe, and K. Kitazawa J. Phys. Chem. A, 105 (2001) 4980.

[38] X.C. Gao, T. Friscic, and L. R. MacGillivray. Angew. Chem. Int. Ed., 43 (2004) 232.

[39] F. Diederich, L. Isaacs, and D. Philp, Chem Soc. Rev., 23 (1994) 243.

[40] R. W. Lof, M. A. van Veenendaal, B. Koopmans, H. T. Jonkman, and G. A. Sawatzky, Phys. Rev. Lett., 68 (1992) 3924.

[41] M. R. Manaa, Chem. Phys. Lett., 400 (2004) 23.